Hirano et al. Translational Medicine Communications (2017) 2:1
DOI 10.1186/s41231-017-0011-y

Translational Medicine Communications

RESEARCH Open Access

Cryoinjury-induced acute myocardial infarction model and ameroid constrictor-induced ischemic heart disease model in adult micro-mini pigs for preclinical studies

Akinori Hirano[1], Jun Fujita[2*], Hideaki Kanazawa[2*], Shinji Kawaguchi[1], Noriko Handa[2], Yoshitake Yamada[3], Shigeo Okuda[3], Shuji Hishikawa[4], Takumi Teratani[4], Satoshi Kunita[4], Shugo Tohyama[2,5], Tomohisa Seki[2], Ryota Tabei[2], Kazuaki Nakajima[2], Yoshikazu Kishino[2], Marina Okada[2], Kazuma Okamoto[1], Hideyuki Shimizu[1], Eiji Kobayashi[4,5] and Keiichi Fukuda[2]

Abstract

Background: Coronary artery diseases (CAD) are the most commonly occurring disorders in the developed countries. Development of new therapeutics and their success in clinical studies require confirmation of therapeutic effects in large animal models. Swine is an ideal animal model because their anatomical features are similar to humans. However, sometimes their large body size hampers translational research, particularly in cell or tissue transplantation procedures for adult stage and long-term observation studies. We have been developing the smallest experimental pig, called micro-mini pigs (MMPs), for regenerative medicine.

Methods: Five- to 14-month-old mature MMPs were used ($n = 15$, body weight: 13.4 ± 2.14 kg). In the acute myocardial infarction (AMI) model, AMI was induced by cryoinjury (CI). In the ischemic heart disease (IHD) model, IHD was induced using an ameroid constrictor (AC) that was applied to the left anterior descending artery, with the diagonal branches ligated. Cardiac function in both models was assessed by magnetic resonance imaging (MRI) with late gadolinium enhancement, and coronary angiography (CAG) was performed to evaluate the collateral arteries. Animals were sacrificed 4 weeks after procedures to evaluate the pathological changes.

Results: On MRI, the ejection fraction in CI-induced AMI models decreased from 57.7 ± 3.2% to 35.8 ± 4.7% (Δ62.2%, $p = 0.012$) ($n = 8$). In contrast, AC also impaired cardiac function, but some pigs did not develop heart failure due to the development of collateral branches (pre: 54.4 ± 4.4%, post: 41.1 ± 8.0%, Δ75.7%, $p = 0.028$ [$n = 7$]). Gadolinium contrast-enhanced MRI and pathological examination confirmed scarring in both models. The proportion of scar area in the left ventricular region of CI-induced AMI models vs. AC-induced IHD models was 19.4% vs. 10.3% ($p = 0.046$) (MRI) and 17.6% vs. 9.2% ($p = 0.046$) (pathology). Immunohistological analysis also showed the presence of marked neovascularization in AC models, which led to greater variation in the impairment of cardiac function.

Conclusions: MMPs are the smallest available swine for experimental use that are suitable for translational research. They allow for long-term observation of adult pathology. Both models of AMI and IHD were successfully established in MMPs. The MMP preclinical heart failure model may accelerate further development of new treatments for CAD.

Keywords: Micro-mini pig, Preclinical model, Coronary artery disease, Heart failure, Acute myocardial infarction, Ischemic heart disease, Cryoinjury, Ameroid constrictor

* Correspondence: jfujita@a6.keio.jp; kanazawa@a5.keio.jp
[2]Department of Cardiology, Keio University School of Medicine, 35 Shinanomachi Shinjuku-ku, Tokyo 160-8582, Japan
Full list of author information is available at the end of the article

Background

Coronary artery disease (CAD) is a leading cause of mortality and mobility in developed countries [1]. Currently, the main therapies for CAD are percutaneous coronary intervention, coronary artery bypass graft surgery, and optimal medical therapies. Despite advances in therapies for CAD over the last half century, mortality among patients with CAD remains high [2]. Severe CAD leads to chronic heart failure (HF), and heart transplantation is the sole effective treatment for terminal stage chronic HF. However, donor shortage is a critical problem globally [3]. In order to address this unmet medical need, various therapeutic strategies must be developed to treat CAD. Small animal models such as mice and rats are suitable for researching the molecular mechanisms of CAD [4]. However, there are large physiological differences between rodents and humans, such as heart rate and heart weight. In contrast, large animal models more closely mimic human diseases in terms of physiological function. New innovative strategies to treat CAD such as gene therapy, stem cell therapy, and pharmacological agents must be assessed for feasibility and safety in preclinical models prior to clinical studies [5–7]. Moreover, the invention of new surgical techniques and mechanical devices such as left ventricular assist devices, artificial hearts, and cardiac assist devices are difficult to test and optimize in small animals. Therefore, pre-clinical studies of these techniques and devices in large animals such as canines, sheep, and swine are strongly recommended before their first usage in human [8]. In particular, swine are ideal for use as a large animal model because their anatomical features, including the coronary arteries, resemble those of the human body [9]. Moreover, unlike dogs, swine do not have pre-formed collateral arteries [9, 10]. The disadvantage of using domestic swine is that they are too large to handle during the course of their growth. In order to observe and evaluate the long-term adult pathology in a CAD animal model, we have been developing a micro-mini pig (MMP) model. MMPs weight up to 10–20 kg in their adult stage, whereas mature miniature pigs weigh 40–50 kg [11]. To our knowledge, there are no reports on established heart disease models with MMPs. In addition, there are no reports demonstrating a direct comparison between CI-induced acute myocardial infarction (AMI) models and AC-induced ischemic heart disease (IHD) models in swine, which are representative models for CAD [12, 13]. CI has been used to make AMI model [14, 15]. Although the myocardial area was injured from the epicardial side, a strong advantage is the ability to control damage to the area [14, 15]. On the other hand, AC gradually constricted the coronary artery to result in ischemia [16].

We evaluated the feasibility of using adult MMPs as preclinical models for AMI and IHD, to aid in the development of new therapies for CAD.

Methods

Animals, anesthesia, and analgesia

Female MMPs ($n = 15$, body weight: 13.44 ± 2.14 kg, Fuji Micra inc, Shizuoka, Japan) aged 5–14 months were used in this study. They underwent general anesthesia with 2–2.5% sevoflurane inhalation, and were pre-medicated with medetomidine chloride (0.08 mg/kg i.m.), midazolam (2 mg/kg, i.m.), and atropine (0.02 mg/kg, i.m.). Analgesia was achieved by administering buprenorphine (0.02 mg/kg, i.v.) during the operations. Prior to the beginning of procedures, systemic heparinization was achieved through intravenous transfusion of heparin at 100 units/kg.

AMI model

Cryoinjury

AMI was induced by CI in 8 female swine (body weight: 14.0 ± 1.7 kg, age 8–14 months), with a stainless rod (Fig. 1d) frozen in liquid nitrogen. The left chest cavity was opened by a left 4th thoracotomy to expose the heart. After administration of systemic heparin (100 units/kg, i.v.), 2 or 3 of the main diagonal branches were ligated with 6–0 prolene sutures. Then, the cryo-rod was pushed to the anterior free wall of the left ventricle for 2 min, moving concurrently with heart beats. Finally, the chest was closed.

IHD model

Ameroid constrictor

IHD was induced by AC in 7 female swine (body weight: 12.8 ± 2.51 kg, age 5–14 months). The left chest cavity was opened by a left 4th thoracotomy to expose the heart. After administration of systemic heparin (100 units/kg, i.v.), 2 or 3 of the main diagonal branches were ligated with 6–0 polypropylene sutures (Ethicon, USA). The wall motion of the left ventricular anterior wall was locked with a stabilizer, and then the AC was implanted in the left anterior descending artery (LAD), ligated around the AC. Finally, the chest was closed.

Cardiac functional assessment with magnetic resonance imaging

Cardiac function was evaluated prior to creation of the models (baseline) and at 4 weeks after the operation, by using 1.5 T magnetic resonance imaging (MRI) (Magnetom Essenza, Siemens Healthcare Sector, Erlangen, Germany) with a phased-array cardiac coil. All images were acquired under apnea with continuous ECG gating, and enhanced by gadolinium enhancement. The left ventricular ejection fraction (LVEF), end systolic volume (LVESV), and end diastolic volume (LVEDV) were assessed and compared between the groups. Myocardial scarring was evaluated by gadolinium contrast injection.

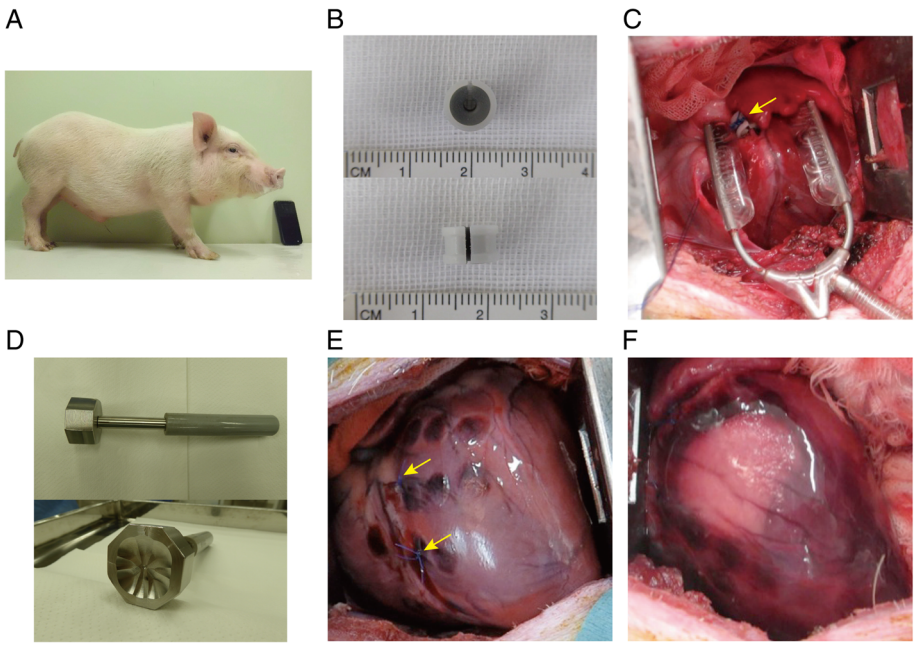

Fig. 1 Cryoinjury (CI) or ameroid constrictor (AC)-induced coronary artery disease (CAD) models. **a** A micro-mini pig (MMP) is a very small swine that weighs 10–20 kg when mature. Here, a MMP is shown together with a smartphone as a comparison of size. **b** Ameroid constrictors (AC) (inner diameter: 2 mm) were used to create a ischemia model. **c** The AC was placed in the proximal region of the left anterior descending artery (LAD). **d** The metallic probe for inducing cryoinjury (CI) to a MMP's heart. **e** Major diagonal branches were ligated under open thoracic surgery. The *yellow arrows* indicate the ligation site. **f** A cold metallic probe was placed at the anterior wall of the porcine heart. The anterior wall was completely ablated by CI after 120 s

Coronary angiography of MMPs

Coronary angiography (CAG) was performed under anesthesia at 4 weeks after the operation. The left and right coronary arteries were separately imaged with contrast medium.

Pathological and Morphometric analysis

After completing the 4-week observation period, the animals were sacrificed by intravenous transfusion of potassium chloride (20 mEq/body) after general anesthesia, and their hearts were explanted. The LV was sectioned into 1-cm-thick short-axis slices to measure infarct size (IS). Transverse ventricular slices were then incubated with 2% TTC (2,3,5-triphenyl tetrazolium chloride) for 20 min at 37 °C to stain viable myocardium. Each slice was imaged digitally to measure the infarct size. Infarct size was expressed as a percent of LV surface area by an image-analysis system (NIH Image J program, available at http://rsb.info.nih.gov/ij).

Immunohistochemistry for angiogenesis

Heart tissues were fixed in 4% paraformaldehyde, embedded in paraffin, and then sections were cut at 6 μm intervals vertical to the long axis of the heart. For immunofluorescence staining, heart tissues were fixed in 4% paraformaldehyde, embedded in an optimal cutting temperature compound, and then snap-frozen in liquid nitrogen. Cryosections were stained with primary antibodies against a cardiomyocyte specific marker (troponin-T (Abcam, Cambridge, UK)), an endothelial cell (EC) marker (von Willebrand factor (vWF) (Abcam)), and a smooth muscle marker (α-smooth muscle actin (SMA) (Dako, Denmark)). Primary antibodies were visualized with fluorescent secondary antibodies. Nuclei were stained with 4',6-diamidino-2-phenylindole dihydrochloride (DAPI) (Invitrogen). All in vitro images were acquired and analyzed by using a fluorescence microscope (Axio Observer; Carl Zeiss Inc., Oberkochen, Germany). After immunofluorescence staining, the area of angiogenesis was quantified by the number of vWF positive cells or SMA positive vessels in the scarred and normal zones.

Growth curve and heart size of MMPs

Body weight of the MMPs was measured at Fuji Micra farm (male: $n = 34$ female: $n = 34$). A MMP and a farm pig were sacrificed to compare their hearts. They were sacrificed by intravenous transfusion of potassium chloride (20 mEq/body) after general anesthesia, and their hearts were explanted.

Statistics

IBM SPSS Advanced Statistics 22 (IBM Inc, Chicago, IL, USA) was used for statistical analyses. Error bars represented the standard deviation (SD). The significance of

differences in cardiac function and scar area between 2 groups was analyzed by non-parametric inferential statistical methods (Mann–Whitney *U* test or Wilcoxon rank sum test, as appropriate for each parameter). The significance of differences between 2 groups in the pathological evaluation of angiogenesis in the scar area was analyzed with Student's *t*-test; $^{*}p < 0.05$ was considered significant.

Results

AMI model with cryoinjury and IHD model with ameroid constrictor

MMPs were small swine, and their body size reached approximately 10–20 kg at the adult stage (Fig. 1a and Additional file 1: Figure S1A). The size of a MMP heart was much smaller than the heart of a farm pig (Additional file 1: Figure S1B). AC (inner cavity diameter was 2.0 mm, appropriate for MRI usage) was chosen to constrict LAD in MMPs (Fig. 1b). Major diagonal branches were ligated after open thoracotomy by 6–0 prolene. The proximal region of LAD was exposed carefully, and the AC was attached to the LAD (Fig. 1c). When a 1.5-mm inner diameter AC was used, it sometimes induced ventricular tachycardia. However, the appropriate AC (2.0 mm inner diameter) did not trigger fatal arrhythmia. AMI models were created with CI. A metallic probe was designed to fit with the anterior wall of MMPs' hearts, so that the central portion of the metallic probe was hollowed out like a flower (Fig. 1d). At first, major diagonal branches were also ligated by 6–0 prolene, while the metallic probe was deeply cooled by liquid nitrogen for 10 min (Fig. 1e). It was pressed against the anterior wall of the beating heart for 120 s (Fig. 1f). Fatal arrhythmia was not observed during the procedure. In both models, animals were gently kept in their pig cages after their chest was closed. No MMPs died after any procedures, and did not die until they were sacrificed.

Cardiac function with MRI

Cardiac function was assessed by cardiac MRI prior to and 1 month after procedures. Systolic function was evaluated by assessing LVEF (Additional file 2: Video S1 and Additional file 3: Video S2). Representative images of the systolic and diastolic ventricles (short axis view) in both models are shown in Fig. 2a and b. The LVEF in normal MMP hearts was 50%–60% ($n = 15$).

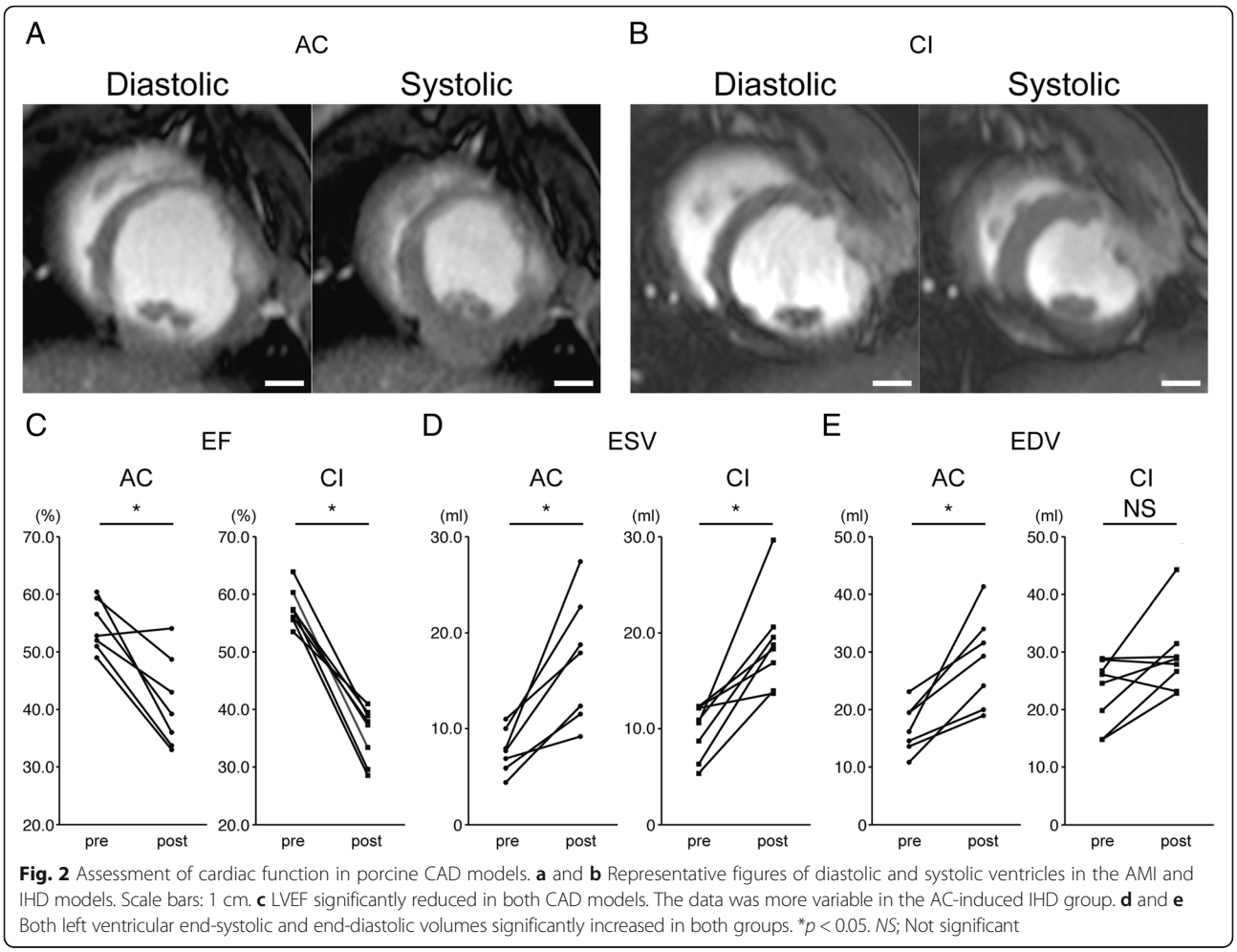

Fig. 2 Assessment of cardiac function in porcine CAD models. **a** and **b** Representative figures of diastolic and systolic ventricles in the AMI and IHD models. Scale bars: 1 cm. **c** LVEF significantly reduced in both CAD models. The data was more variable in the AC-induced IHD group. **d** and **e** Both left ventricular end-systolic and end-diastolic volumes significantly increased in both groups. $^{*}p < 0.05$. *NS*; Not significant

The LVEF in MMP hearts in the AC group was 41.1 ± 8.0% ($n = 7$). In contrast, LVEF at 1 month after CI was 35.8 ± 4.7% ($n = 8$). The LVEF measured in the AC model tended to be more variable compared to the LVEF measured in CI-induced AMI models (Fig. 2c). LVESV and LVEDV were also evaluated as part of volumetric analysis (Fig. 2d and e). A month after induction of AMI or IHD in the 2 models, the left ventricles appeared dilated as a result of left ventricular remodeling. (Fig. 2d and e).

Evaluation of scar area in AMI and IHD models

Late gadolinium enhancement of MRI was used to confirm the scar area in the LV anterior wall. A broad scar area is visible on the images of MMP hearts in the CI-induced AMI model (Fig. 3a). The proportion of scar area in the AMI model (CI group) was 19.4 ± 5.9%. The average size of the scar area was larger in the AMI model compared to the IHD model. Moreover, in the AC-induced IHD model, the proportion of the scar area was more variable, at 10.3 ± 7.7% (Fig. 3b).

Cardiac sections were stained with TTC for pathological evaluation of the infarcted lesions, and morphometric analysis was performed in both models. In the AMI models, the left anterior myocardium was ablated from the epicardium to the inner layers, which resulted in a thinner scar area (Fig. 3c). The proportion of scar area in the AMI model was 17.6 ± 4.1%, as determined by TTC staining. In line with the results of late gadolinium enhanced area, the average size of the scar area was larger in the CI-induced AMI model, and the proportion of scar area in the IHD models was more variable, at 9.17 ± 8.1% (Fig. 3d). Cardiac sections were also stained with hematoxylin and eosin, as well as azan stain. Microscopic

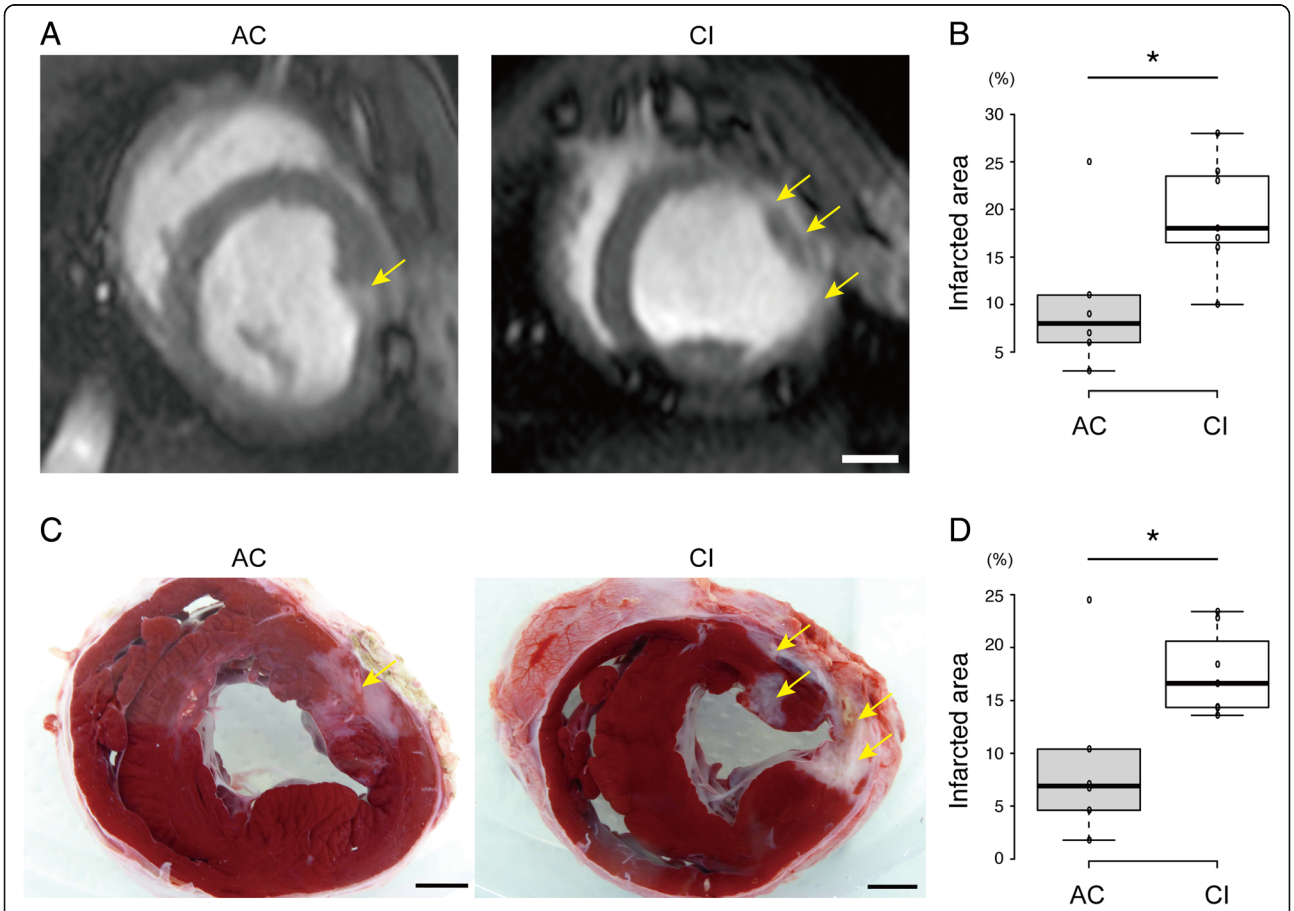

Fig. 3 Morphological evaluation of infarcted hearts in CI or AC- induced CAD models. **a** Representative figures of late gadolinium enhanced scar area in both CAD models. The yellow arrows indicate that the scar area as confirmed by gadolinium staining. **b** Late gadolinium enhancement reveals that the scar area of AC-induced IHD models are more variable compared to the scar area found in CI-induced AMI models. **c** 2,3,5-Triphenyl-2H-tetrazolium Chloride (TTC) staining of infarcted hearts was performed to evaluate the scar area. The CI-induced AMI model also showed transmural MI. The *yellow arrows* indicate the scar area, identified by the absence of TTC staining. **d** Morphometric analysis also confirmed that the scar area of AC-induced IHD models is more variable compared to the scar areas found in the CI-induced AMI models. *$p < 0.05$

pathology confirmed that both CAD models successfully induced AMI (Fig. 4).

These data confirmed that the CI-induced AMI model was a more stable method to create a HF model.

AC-induced IHD model strongly induced angiogenesis

In the IHD model, AC occluded the proximal region of the LAD (Fig. 5a). Anatomical features of coronary arteries in 4 AC-induced IHD models were evaluated by CAG. The proximal LAD was totally occluded in 3 of 4 pigs (Fig. 5b and Additional file 4: Video S3). One pig had 75% stenosis of the pLAD on CAG (Fig. 5c and Additional file 5: Video S4). In the hearts from the AC-induced IHD model, collateral arteries developed in the distal region of the LAD (arrows in Fig. 5b and c and Additional file 4: Video S3 and Additional file 5: Video S4). In contrast, no obvious collateral arteries developed in the hearts from the CI-induced AMI model (Fig. 5d and Additional file 6: Video S5). These data indicated that AC, which induced ischemia, resulted in various degrees of occlusion of the LAD, and caused collateral arteries to develop.

Pathological evaluation of scar area for angiogenesis in AMI and IHD models

Sections were also stained with vWF to evaluate microvascular angiogenesis. Increased vasculature was identified in the scar area of hearts in the IHD models ($p < 0.05$; Fig. 6a and b). Immunohistochemistry with α-SMA also confirmed that increased angiogenesis was occurring in the scar area in AC-induced IHD models ($p < 0.05$; Fig. 6c and d). The pathology data correlated with the results of CAG. These data confirmed that the AC-induced IHD model contained more vasculature in the scar area, but a smaller area of scarring. This resulted in variation in the exacerbation of HF.

Discussion

We succeeded in establishing models of AMI and IHD in adult MMPs by using CI and AC, in combination with

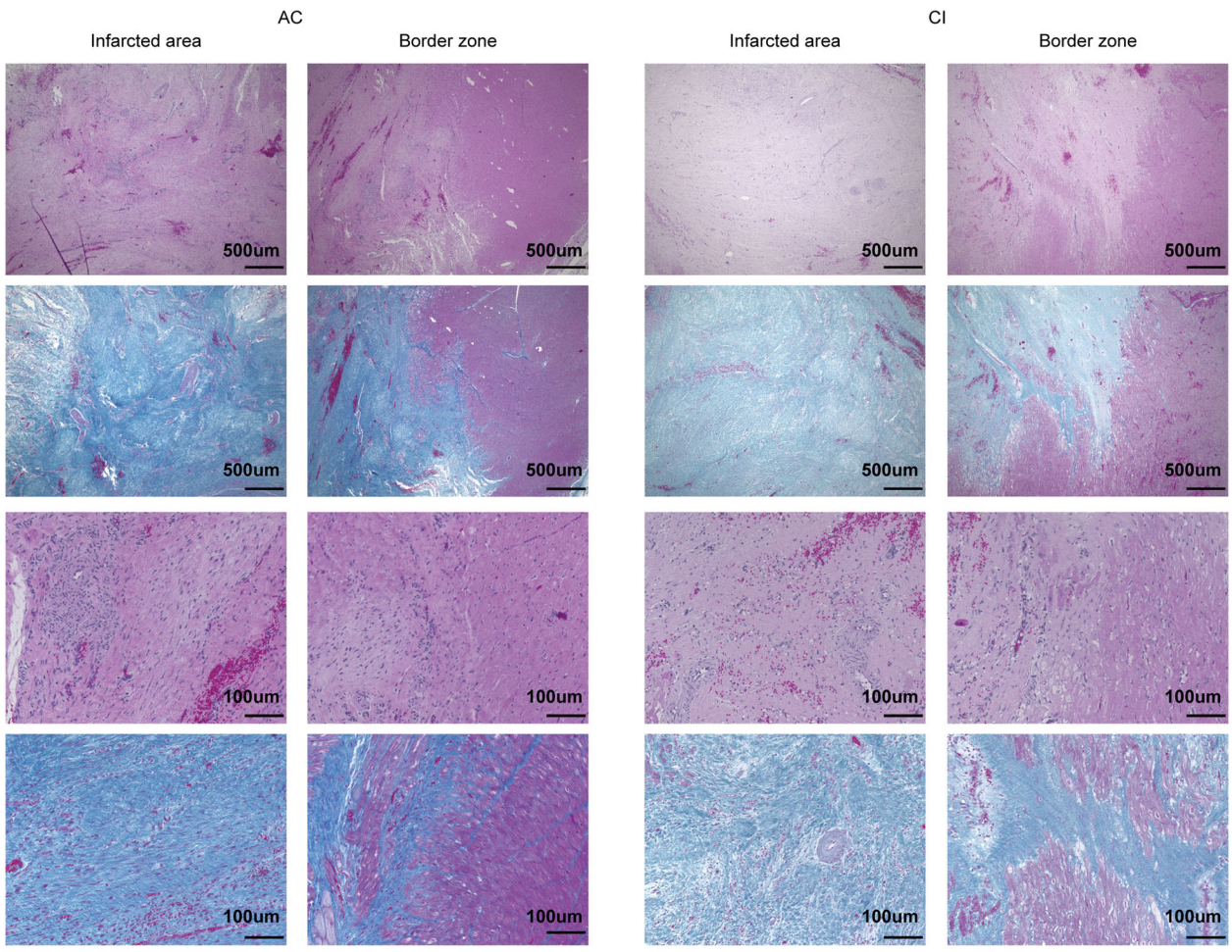

Fig. 4 Pathological examination and fibrosis of porcine CAD models. Hematoxylin and eosin staining reveals a clearly scar area in both CAD models. Azan staining confirmed fibrosis in the scar area in both models

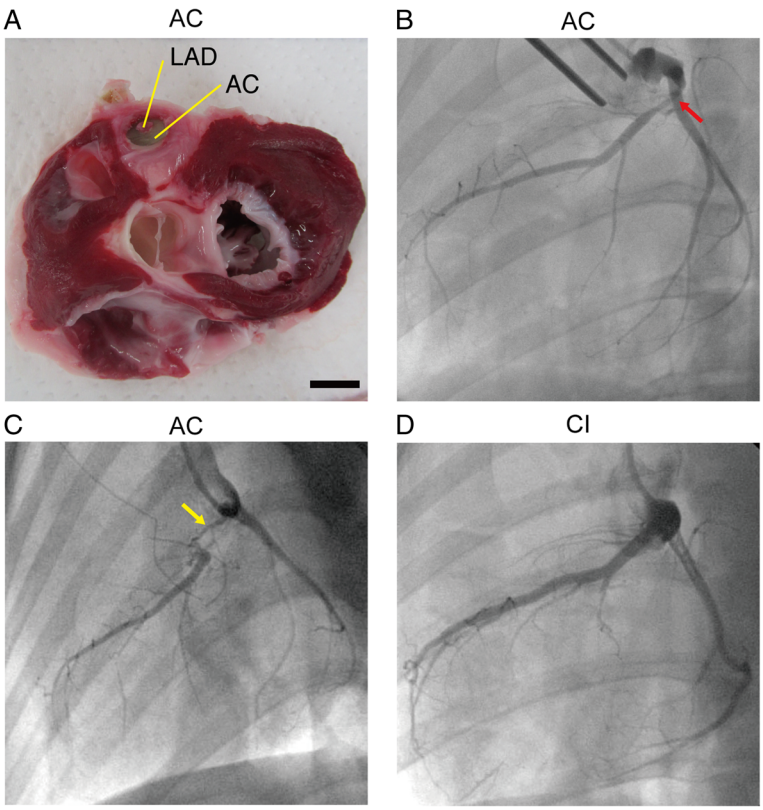

Fig. 5 Coronary angiography for CI or AC- induced CAD models. **a** AC apparently occluded the proximal region of the LAD. Scale bar: 1 cm. LAD; left anterior descending artery. AC; ameroid constrictor. **b** and **c** Representative figures with coronary angiography (CAG) of AC-induced infarcted hearts. AC sometimes failed to occlude the artery completely (*red arrow*). Note: functional collateral arteries usually developed to bridge collateral from left main trunk artery to the LAD (*yellow arrows*). **d** Representative figure of CAG in a CI-induced infarcted heart. There is no obvious development of a collateral artery

diagonal branch ligation. Both models clearly demonstrated decreased cardiac function a month after induction of AMI or IHD. In particular, CI consistently decreased cardiac function to 25–35% of EF, as determined by MRI. Pathological examination showed that our method solved the technical problem of inducing CI, as it is sometimes difficult to create a transmural AMI model. The AC-induced IHD models caused significant angiogenesis and development of collateral vasculature, which hampered stable chronic HF.

In humans, CAD usually develops in adults, but conventional swine CAD models have used immature domestic pigs or miniature pigs. In their adult stage, domestic pigs will reach weights exceeding 300 kg. Younger domestic pigs or miniature pigs are often used for medical research worldwide, but it is difficult to observe these animals over a long period due to their growth. Even miniature pigs in their adult stage often weigh over 50 kg, so these models are difficult to manage for translational research. MMPs are the smallest swine, but larger than a beagle dog, and thus are suitable for use in experiments. Therefore, MMPs have a size that allows for easy handling, and they are appropriate for use in translational research, even at mature ages. Furthermore, it is relatively easy to scale up the dose of therapeutic agents for systemic administration in MMPs. Because their use enables long-term observation, induction of traditional cardiovascular risk factors, such as hypertension and diabetes mellitus, can be a future focus of research with MMPs.

Several CAD models were reported in swine. Microembolization, coronary artery ligation, balloon inflation, coil deployment, AC, and CI have been used for porcine MI/reperfusion models [12, 17–21]. Each model has advantages and disadvantages. In coronary ligation of the LAD, it is difficult to induce infarction areas of the same size. If the coronary arteries are occluded at the LAD, it often causes ventricular fibrillation which results in sudden death [22]. Coil embolization and balloon inflation is needed to assess the anatomy of coronary arteries through CAG, in order to select the appropriate arteries because occlusion of the proximal arteries leads to ventricular fibrillation. The complexity of these techniques restricts the institution to create swine models of

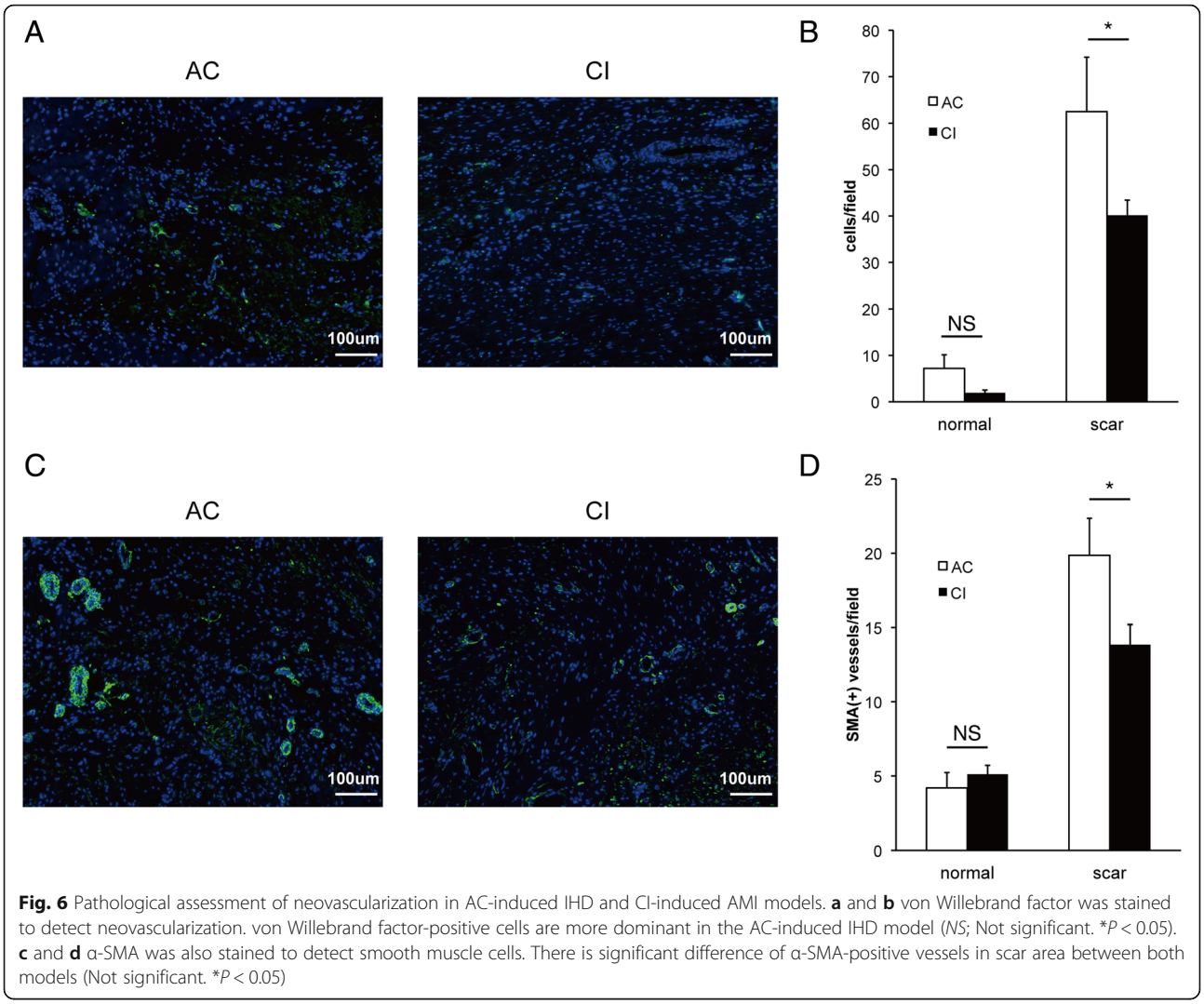

Fig. 6 Pathological assessment of neovascularization in AC-induced IHD and CI-induced AMI models. **a** and **b** von Willebrand factor was stained to detect neovascularization. von Willebrand factor-positive cells are more dominant in the AC-induced IHD model (*NS*; Not significant. $^{*}P < 0.05$). **c** and **d** α-SMA was also stained to detect smooth muscle cells. There is significant difference of α-SMA-positive vessels in scar area between both models (Not significant. $^{*}P < 0.05$)

AMI. We found that even with the use of CAG, microembolization frequently resulted in ventricular fibrillation and the mortality was 75% ($n = 4$). Therefore, LCX was often used as the main target vasculature for these procedures. However, LCX occlusion induces only small AMIs, and it resulted in lateral-posterior wall infarction. Consequently, it is difficult to establish significant HF from the small infarction area caused by LCX occlusion. Compared to anterior wall infarctions, the lateral-posterior infarcted area was also difficult to approach for treatment, such as with cell transplantation. Therefore, LAD occlusion is necessary to establish significant HF via CAD, for translational research.

Because of such difficulties in creating swine models of AMI, ACs were popular to make a IHD model [23], even though LCX occlusion was more popular than LAD, as well. AC squeezes a coronary artery gradually for approximately 1 month, which eventually leads to ischemic cardiomyopathy. The longer observation of AC-induced IHD will be also useful to study the IHD-induced remodeling effect. It is difficult to control the infarction size through this technique because collateral arteries develop in some swine, and significant HF cannot be established [17]. In contrast, the CI-induced AMI model is a very popular technique for small animals, but not in swine, because of the large size of the pig heart. CI would have to be conducted several times, which makes it difficult to control the size of infarction. The heart size of a MMP measured 5 cm in diameter (70 g), so the MMPs were suitable for CI. Only one time procedure was enough to make AMI model. The other challenge in creating the CI-induced AMI model was the difficulty in inducing transmural infarction. The additional ligation of diagonal branches was very effective to induce transmural infarction but not ventricular tachycardia. In the CI-induced AMI model, collateral artery development was poor and there was significantly less angiogenesis compared to the AC-induced IHD model. Such a distinct difference in

vascularization suggests that the CI model established stable chronic HF in swine.

Female pigs were used for this study because our CAD models were experimentally induced. The characteristics of CAD in women are different from those in men. Women have more severe CAD risk factors, a higher prevalence of angina, a lower burden of obstructive CAD, and a poorer prognosis [24]. Therefore, sex is an important factor, if traditional CV risk factors and long-term prognosis are the focus of study.

Conclusions

AMI and IHD models were established in MMPs. MMPs are useful animals for translational research to treat CAD. These techniques and suitable animals for translational research will allow for the study of new therapeutic strategies for severe HF, such as stem cell therapies and gene therapy, and advance the development of new device and surgical procedures.

Limitations of the study

MMPs were used for all experiments; thus the results may differ from those obtained using other swine. AC-induced IHD were different from cardiovascular risk factor-induced IHD, so they could have different pathogenesis. As only females were used in this study, research on sex-specific characteristics of CAD requires use of both male and female pigs. The observation period was 4 weeks in this study, and longer observation will be necessary to investigate the remodeling effect of CAD.

Additional files

Additional file 1: Figure S1. (A) Growth curves of the MMPs. Both males and female swine weighed 10–20 kg at 6 months after birth. (B and C) The heart size of MMP was much smaller than that of a farmer pig. (PNG 1549 kb)

Additional file 2: Video S1. Cardiac MRI of AC-induced IHD model. (MOV 7402 kb)

Additional file 3: Video S2. Cardiac MRI of CI-induced AMI model. (MOV 6641 kb)

Additional file 4: Video S3. CAG of AC-induced IHD model (AC completely occluded the artery). (MOV 4582 kb)

Additional file 5: Video S4. CAG of AC-induced IHD model (AC failed to occlude the artery). (MP4 6070 kb)

Additional file 6: Video S5. CAG of CI-induces AMI model. (MOV 1841 kb)

Abbreviations

AC: Ameroid constrictor; AMI: Acute myocardial infarction; CAD: Coronary artery disease; CAG: Coronary angiography; CI: Cryoinjury; DAPI: 4',6-diamidino-2-phenylindole dihydrochloride; EC: Endothelial cell; EDV: End diastolic volume; EF: Ejection fraction; ESV: End systolic volume; HF: Heart failure; IHD: Ischemic heart disease; LAD: Left anterior descending artery; LCX: Left circumflex artery; LV: Left ventricle; MMP: Micro-mini pig; MRI: Magnetic resonance image; SD: Standard deviation; SMA: Smooth muscle actin; vWF: von Willebrand factor

Acknowledgements

The authors thank Natsuko Hemmi, Rei Ohno, Chihana Fujita, Sayaka Kanaami, Miho Yamaguchi, Yoshiko Miyake, and Yukitoshi Makimura for technical assistance. The authors are grateful to Takashi Nishimura and Noriaki Satake for measuring the body weight of MMPs (Fuji Micra).

Funding

This work was supported by the Highway Program for Realization of Regenerative Medicine (16bm0504006h0006) from Japan Agency for Medical Research and Development (to KF).

Availability of data and materials

Please contact author for data requests.

Authors' contributions

JF and HK designed the experiments. AH performed the majority of the experiments. AH, S Kawaguchi and HK performed the coronary angiography. EK supervised the creation of the MMP strain. NH, TT, S Kunita, and SH supported all the animal experiments. JF, HK, KO, HS, EK, and KF supervised the experiments. YY and SO analyzed the MRI data. AH, ST, TS, RT, KN, YK and MO analyzed and interpreted the data. JF wrote the first draft of the manuscript. AH, JF, HK, EK and KF revised the manuscript. All authors read and approved the final manuscript.

Competing interests

EK received an honorarium as a supervisor for creating the MMP strain (2012–2013). KF is a cofounder of Heartseed Inc.

Consent for publication

Not applicable.

Ethics approval and consent to participate

The experimental protocol was approved by the Sub-committee on Animal Care and the Institutional Review Board of Keio University and Jichi Medical University. All animals received humane care in accordance with the Principles of Laboratory Animal Care and the Guide for the Care and Use of Laboratory Animals Research, U.S.A. (http://www.nap.edu/catalog/5140.html).

Author details

[1]Department of Cardiovascular Surgery, Keio University School of Medicine, 35 Shinanomachi Shinjuku-ku, Tokyo 160-8582, Japan. [2]Department of Cardiology, Keio University School of Medicine, 35 Shinanomachi Shinjuku-ku, Tokyo 160-8582, Japan. [3]Department of Diagnostic Radiology, Keio University School of Medicine, 35 Shinanomachi Shinjuku-ku, Tokyo 160-8582, Japan. [4]Center for Development of Advanced Medical Technology, Jichi Medical University, 3311-1 Yakushiji, Shimotsuke-shi, Tochigi 329-0498, Japan. [5]Department of Organ Fabrication, Keio University School of Medicine, 35 Shinanomachi Shinjuku-ku, Tokyo 160-8582, Japan.

Received: 29 December 2016 Accepted: 10 January 2017
Published online: 08 February 2017

References

1. Mozaffarian D, Benjamin EJ, Go AS, Arnett DK, Blaha MJ, Cushman M, de Ferranti S, Despres JP, Fullerton HJ, Howard VJ, et al. Heart disease and stroke statistics-2015 update: a report from the american heart association. Circulation. 2015;131:e29–e322.
2. Nabel EG, Braunwald E. A Tale of Coronary Artery Disease and Myocardial Infarction. N Engl J Med. 2012;366:54–63.
3. Lund LH, Edwards LB, Kucheryavaya AY, Benden C, Christie JD, Dipchand AI, Dobbels F, Goldfarb SB, Levvey BJ, Meiser B, et al. The registry of the International Society for Heart and Lung Transplantation: thirty-first official adult heart transplant report–2014; focus theme: retransplantation. J Heart Lung Transplant. 2014;33:996–1008.
4. Rafiq K, Kolpakov MA, Seqqat R, Guo J, Guo X, Qi Z, Yu D, Mohapatra B, Zutshi N, An W, et al. c-Cbl inhibition improves cardiac function and survival in response to myocardial ischemia. Circulation. 2014;129:2031–43.
5. Byrne MJ, Power JM, Preovolos A, Mariani JA, Hajjar RJ, Kaye DM. Recirculating cardiac delivery of AAV2/1SERCA2a improves myocardial function in an experimental model of heart failure in large animals. Gene Ther. 2008;15:1550–7.

6. Kanazawa H, Tseliou E, Malliaras K, Yee K, Dawkins JF, De Couto G, Smith RR, Kreke M, Seinfeld J, Middleton RC, et al. Cellular Post-Conditioning: Allogeneic Cardiosphere-Derived Cells Reduce Infarct Size and Attenuate Microvascular Obstruction When Administered After Reperfusion in Pigs With Acute Myocardial Infarction. Circ Heart Fail. 2015;8:322–32.
7. Ogura Y, Ouchi N, Ohashi K, Shibata R, Kataoka Y, Kambara T, Kito T, Maruyama S, Yuasa D, Matsuo K, et al. Therapeutic impact of follistatin-like 1 on myocardial ischemic injury in preclinical models. Circulation. 2012;126:1728–38.
8. Dixon JA, Spinale FG. Large animal models of heart failure: a critical link in the translation of basic science to clinical practice. Circ Heart Fail. 2009;2:262–71.
9. Weaver ME, Pantely GA, Bristow JD, Ladley HD. A quantitative study of the anatomy and distribution of coronary arteries in swine in comparison with other animals and man. Cardiovasc Res. 1986;20:907–17.
10. Scheel KW, Wilson JL, Ingram LA, McGehee L. The septal artery and its collaterals in dogs with and without circumflex occlusion. Am J Physiol. 1980;238:H504–514.
11. Kobayashi E, Hishikawa S, Teratani T, Lefor AT. The pig as a model for translational research: overview of porcine animal models at Jichi Medical University. Transplant Res. 2012;1:8.
12. Yang Y, Sun J, Gervai P, Gruwel ML, Jilkina O, Gussakovsky E, Yang X, Kupriyanov V. Characterization of cryoinjury-induced infarction with manganese-and gadolinium-enhanced MRI and optical spectroscopy in pig hearts. Magn Reson Imaging. 2010;28:753–66.
13. Harada K, Friedman M, Lopez JJ, Wang SY, Li J, Prasad PV, Pearlman JD, Edelman ER, Sellke FW, Simons M. Vascular endothelial growth factor administration in chronic myocardial ischemia. Am J Physiol. 1996;270: H1791–1802.
14. Jensen JA, Kosek JC, Hunt TK, Goodson 3rd WH, Miller DC. Cardiac cryolesions as an experimental model of myocardial wound healing. Ann Surg. 1987;206:798–803.
15. Ciulla MM, Paliotti R, Ferrero S, Braidotti P, Esposito A, Gianelli U, Busca G, Cioffi U, Bulfamante G, Magrini F. Left ventricular remodeling after experimental myocardial cryoinjury in rats. J Surg Res. 2004;116:91–7.
16. Wunsch M, Sharma HS, Markert T, Bernotat-Danielowski S, Schott RJ, Kremer P, Bleese N, Schaper W. In situ localization of transforming growth factor beta 1 in porcine heart: enhanced expression after chronic coronary artery constriction. J Mol Cell Cardiol. 1991;23:1051–62.
17. Roth DM, Maruoka Y, Rogers J, White FC, Longhurst JC, Bloor CM. Development of coronary collateral circulation in left circumflex Ameroid-occluded swine myocardium. Am J Physiol. 1987;253:H1279–1288.
18. Fujiwara H, Ashraf M, Sato S, Millard RW. Transmural cellular damage and blood flow distribution in early ischemia in pig hearts. Circ Res. 1982;51:683–93.
19. Dib N, Diethrich EB, Campbell A, Gahremanpour A, McGarry M, Opie SR. A percutaneous swine model of myocardial infarction. J Pharmacol Toxicol Methods. 2006;53:256–63.
20. Kumar A, Beohar N, Arumana JM, Larose E, Li D, Friedrich MG, Dharmakumar R. CMR imaging of edema in myocardial infarction using cine balanced steady-state free precession. JACC Cardiovasc Imaging. 2011;4:1265–73.
21. Galvez-Monton C, Prat-Vidal C, Diaz-Guemes I, Crisostomo V, Soler-Botija C, Roura S, Llucia-Valldeperas A, Perea-Gil I, Sanchez-Margallo FM, Bayes-Genis A. Comparison of two preclinical myocardial infarct models: coronary coil deployment versus surgical ligation. J Transl Med. 2014;12:137.
22. Muller CA, Opie LH, Hamm CW, Peisach M, Pineda CA, Thandroyen FT. Verapamil and tiapamil in prevention of ventricular fibrillation in pigs with coronary ligation. Comparative effects on left ventricular function. Circulation. 1988;78:227–32.
23. Kawamoto A, Tkebuchava T, Yamaguchi J, Nishimura H, Yoon YS, Milliken C, Uchida S, Masuo O, Iwaguro H, Ma H, et al. Intramyocardial transplantation of autologous endothelial progenitor cells for therapeutic neovascularization of myocardial ischemia. Circulation. 2003;107:461–8.
24. Garcia M, Mulvagh SL, Merz CN, Buring JE, Manson JE. Cardiovascular Disease in Women: Clinical Perspectives. Circ Res. 2016;118:1273–93.